Optical Pumping of Electron Spins in Quantum Dot Ensembles

I. Kleinjohann, A. Fischer, N. Jäschke, F. B. Anders

published in

NIC Symposium 2020
M. Müller, K. Binder, A. Trautmann (Editors)

Forschungszentrum Jülich GmbH,
John von Neumann Institute for Computing (NIC),
Schriften des Forschungszentrums Jülich, NIC Series, Vol. 50,
ISBN 978-3-95806-443-0, pp. 247.
http://hdl.handle.net/2128/24435

Optical Pumping of Electron Spins in Quantum Dot Ensembles

Iris Kleinjohann, Andreas Fischer, Natalie Jäschke, and Frithjof B. Anders

Lehrstuhl für theoretische Physik II, Fakultät Physik,
Technische Universität Dortmund, 44221 Dortmund, Germany
E-mail: {*iris.kleinjohann,frithjof.anders*}*@tu-dortmund.de*

We use the central spin model to analyse optical pumping of singly charged quantum dots. An exact quantum mechanical approach is employed to calculate the impact of several million laser pulses. The periodical excitation imprints on the system and the electron spin polarisation refocuses directly before each pulse. Our calculations link the non-monotonic behaviour of the revival amplitude as function of the external magnetic field found in experiments to the nuclear Larmor precession. Furthermore, we extend our model to a cluster of coupled central spin models to investigate long-range spin-spin interactions in quantum dot ensembles. A semiclassical approach handles the large amount of spins. By means of the cluster approach, we provide an understanding of the electron spin dephasing at different external magnetic fields and spectral widths of the optical excitation. Our model reveals the counterbalancing effects generating a constant dephasing time in dependence of the spectral laser width in experiment.

1 Introduction

Coherent control of electron spins in quantum dot (QD) ensembles appears to be a promising root for realisations of quantum information processing. The confined electron in a singly charged semiconductor QD has limited overlap with the environment leading to a long spin life-time. The major source of decoherence of the electron spin results from the Overhauser field generated by the hyperfine coupling to the surrounding nuclear spins.

A substantial revival amplitude of electron spin polarisation[1–5] arises during the periodic application of laser pump pulses onto an ensemble of QDs subject to a constant magnetic field perpendicular to the optical axis. A resonance condition for the electron spin precession imposes a peaked non-equilibrium distribution of the Overhauser field component parallel to the external magnetic field that emerges from the initial Gaussian distribution. This imprint on the nuclear spins is robust against decoherence mechanisms and thus, is still accessible after minutes without optical driving[5, 6] opening the door to long memory times.

The dephasing of the electron spin polarisation generated by optical excitation depends on various counterbalancing mechanism. One of the dominant effects, aside of the hyperfine interaction and varying electron g factors, is the effective coupling between electron spins of different QDs on the sample. This inter QD interaction was indicated in two-colour pump-probe experiments[7] and presents the opportunity to correlate the spin dynamics of different QDs via tailored optical excitation.

2 Modelling of the System

The Fermi contact hyperfine interaction between the electron spin localised in a self-assembled QD and the surrounding nuclear spin bath provides the largest contribution

to electron spin dephasing[8] in a single semiconductor QD. Other interactions such as the nuclear dipole-dipole interactions are several orders of magnitude smaller and, therefore, will be neglected in the following.[8–10] The Hamiltonian of the central spin model[11] (CSM) accounts for the effect of the external magnetic field $\vec{B}_{\rm ext}$ on electron $\vec{S}$ and nuclear spins $\vec{I}_k$, as well as for the hyperfine interaction (see Fig. 1 (a) for a sketch)

$$\hat{H}_{\rm CSM} = g_e \mu_B \vec{B}_{\rm ext} \hat{\vec{S}} + \sum_{k=1}^{N} g_N \mu_N \vec{B}_{\rm ext} \hat{\vec{I}}_k + \sum_{k=1}^{N} A_k \hat{\vec{I}}_k \hat{\vec{S}} \tag{1}$$

The ratio between nuclear and electronic Zeemann energy, which on average has a value $z = g_N \mu_N / (g_e \mu_B) = 1/800$ in InGaAs QDs, depends on the electron and the nuclear g factor, g_e and g_N, as well as on the respective magnetic momenta, μ_B and μ_N. In a nuclear spin bath of size N, we label the hyperfine coupling constant for the k-th nuclear spin A_k. The nuclear spins weighted by these coupling constants generate the Overhauser field,

$$\hat{\vec{B}}_N = (g_e \mu_B)^{-1} \sum_k A_k \hat{\vec{I}}_k \tag{2}$$

an effective magnetic field acting on the electron spin. In combination with the external magnetic field, it determines the electron Larmor precession. The fluctuations of the Overhauser field, $\langle \vec{B}_{\rm N}^2 \rangle$, in absence of an external magnetic field define a characteristic time scale of the system $(T_N^*)^{-2} = \sum_k A_k^2 \langle \vec{I}_k^2 \rangle$ governing the short-time electron spin dephasing which is typically a few ns in real systems.

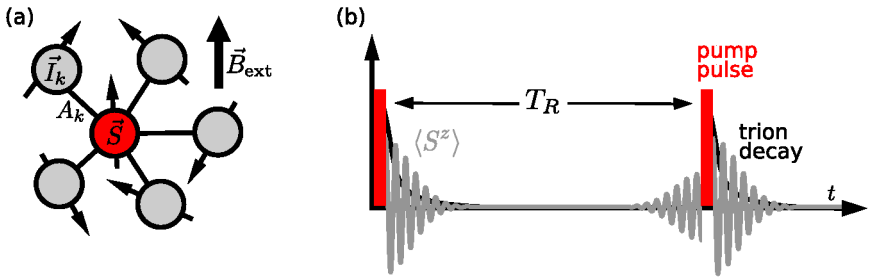

Figure 1. (a) In the central spin model (CSM) the electron spin $\vec{S}$ couples to a bath of nuclear spins $\vec{I}_k$. The external magnetic field $\vec{B}_{\rm ext}$ acts on electron and nuclear spins. (b) Pump pulses periodically generate electron spin polarisation $\langle S^z \rangle$ via trion excitation. The generated polarisation dephases while oscillating due to the magnetic field. As a result of synchronisation with the excitation periodicity, a revival of electron polarisation occurs before each laser pulse.

2.1 Optical Pumping

In optical pump-probe experiments, additional to the electron an electronic particle-hole excitation is created. The bound three particle state is called a trion, and its radiative decay is included in a Lindblad equation for the density operator $\hat{\rho}$ of the electron-nuclear spin system,

$$\dot{\hat{\rho}}(t) = -i \left[\hat{H}, \hat{\rho} \right] - \gamma \left(\hat{\rho} \hat{s} \hat{s}^\dagger + \hat{s} \hat{s}^\dagger \hat{\rho} - 2 \hat{s}^\dagger \hat{\rho} \hat{s} \right) \tag{3}$$

The operators $\hat{s} = |T\rangle\langle\uparrow|$, $\hat{s}^\dagger = |\uparrow\rangle\langle T|$ incorporate the transitions from the spin $|\uparrow\rangle$ to the trion state $|T\rangle$ and *vice versa*. The corresponding transition rate is typically $\gamma = 10\,\mathrm{ns}^{-1}$ in real systems. In the Hamiltonian $\hat{H}$ we include the CSM and the trion state. A scheme of the time scales in the periodically driven system with short optically pulses is shown in Fig. 1 (b). This dynamics can be treated in two ways, either with an exact quantum mechanical description or a semiclassical approach.

When focusing on quantum mechanical effects, we restrict ourselves to a small nuclear spin bath and calculate[12] the exact time evolution of the density operator. To compensate for the relatively small number of nuclear spins ($N = 6 - 8$), the hyperfine coupling constants A_k are drawn from their distribution function in large systems, and the results of N_C different realisations are averaged at the end. Typically about $N_C = 100$ configurations are used which allows for massive parallelisation of the calculations. The calculation of the time dependent density operator $\hat{\rho}(t)$, which consists of mainly matrix multiplications, is parallelised over all cores on one node and N_C nodes are used for a run. With that approach we can apply about 20 million laser pulses to the system with a repetition time of $T_R = 13.2$ ns and span 11 orders of magnitude in time, from the pulse duration of about 4 ps to 0.24 s in real time.

2.2 Semiclassical Approach

We also developed a hybrid approach[3] to combine the quantum description required to capture the effect of the periodic laser pulses and the consecutive trion decay. This semiclassical approach enables the treatment of larger nuclear spin baths[13] than in the quantum mechanical approach.

To this end, we incorporate[3] the quantum mechanical laser pulse by a mapping $\vec{S}_{\mathrm{prior}} \rightarrow \vec{S}_{\mathrm{after}}$ using a unitary time evolution operator and treat the Lindblad equation in the hybrid equation of motion (EOM). We extended[14] the EOM in our semiclassical approach to a coupled cluster theory comprising N_{QD} QDs labelled $i = 1, \ldots, N_{QD}$

$$\frac{\mathrm{d}}{\mathrm{d}t}\vec{S}^{(i)}(t) = \left(\vec{b}_T^{(i)} + g_e^{(i)}\vec{B}_{\mathrm{ext}}\right) \times \vec{S}^{(i)}(t) + \gamma P_T^{(i)}(0)\vec{\mathrm{e}}_z e^{-2\gamma t} \tag{4a}$$

$$\frac{\mathrm{d}}{\mathrm{d}t}\vec{I}_k^{(i)} = \left(A_k^{(i)}\vec{S}^{(i)} + z\vec{B}_{\mathrm{ext}}\right) \times \vec{I}_k^{(i)} \tag{4b}$$

$$\vec{b}_T^{(i)} = \sum_{k=1}^{N} A_k^{(i)}\vec{I}_k^{(i)} + \sum_{j\neq i} J_{ij}\vec{S}_j(t) \tag{4c}$$

with classical spin vectors and the probability of trion occupation P_T. The coupling between electron spins of different QDs, i and j, is named J_{ij}. Furthermore, we take into account different electronic g factors as well as off-resonant pumping caused by the mismatch between the trion excitation energy and the laser frequency.

In the semiclassical simulations, averaging results of various initial classical spin states mimics the quantum mechanical expectation value according to a saddle-point approximation.[13] Up to $N_C = 10^6$ configurations provide highly accurate numerical results. Each computing core handles 32 of these configurations simultaneously to enable vectorisation in 99 % of the program loops. The distribution of the independent configurations over several thousand cores is realised via MPI parallelisation.

3 Signatures of Long-Range Spin-Spin Interactions in an (In,Ga)As Quantum Dot Ensemble

In a two-colour spin pumping experiment[7] evidence was compiled that different QDs are coupled by a long-range spin-spin interaction of unknown origin. The experimental data are consistent with the assumption of a time independent Heisenberg term between pairs of electron spins localised in distinct QDs.

We benchmarked our approach by the simulation of a two size cluster ($N_{QD} = 2$) targeting the understanding of a two colour laser pumping experiment[7] that demonstrated the dependency of the decay time and the phase shifts on the delay time between pump pulses of different colours, acting on different QDs. We find that the theory is able to excellently reproduce the experimental results and establish that the effective spin-spin interaction is long-ranged and time constant. Our results disputes the original interpretation of the experimental paper[7] speculating about an optical Ruderman-Kittel-Kasuya-Yosida interaction (RKKY).

Recently, we extended the calculations to a cluster of up to $N_{QD} = 10$ QDs representing different sub-ensembles with comparable trion excitation energies. Laser pulses modelled by a Gaussian shape with spectral width ΔE have been used. Furthermore, we took into account a Gaussian distribution of electronic g factors and trion excitation energies whose properties have been determined by experiments using the photoluminescence spectra[15] of the QD ensemble. When investigating the dephasing of the electron spin polarisation after a laser pulse (see Fig. 2 (a)) we find three contributing mechanism. The dephasing arising due to the hyperfine coupling is governed by the dephasing time T_N^* encountered before. Additionally, the electron g factor distribution produces varying Larmor frequencies in the QD ensemble. The third contribution is ascribed to the interaction of an electron spin with surrounding unpolarised electron spins in other QDs. Combining these mechanism, the ensemble averaged dephasing time T^* of the electron spin polarisation, as measured in experiments, is obtained and analysed.

In Fig. 2 (b), we compare the experimental data with the calculated values of T^* for an averaged Heisenberg coupling between electron spins $\overline{J} = 0.4\,\mathrm{ns}^{-1}$. The value $\overline{J}$ reproducing the experimental features best is almost a factor 4 smaller than the value $J \approx 1\,\mu\mathrm{eV} \approx 1.5\,\mathrm{ns}^{-1}$ reported in Ref. 7. This smaller value of $\overline{J}$ is a consequence of modelling the ensemble by a cluster of ten QDs instead of a pair only.

The magnetic field dependence of the dephasing time T^* at a fixed spectral width $\Delta E = 1.5\,\mathrm{meV}$ is depicted in Fig. 2 (c). The numerical calculations with $\overline{J} = 0.4\,\mathrm{ns}^{-1}$ (triangles) as well as the experimental measurements (x markers) display a decrease of the dephasing time with increasing external magnetic field. For our choice of parameters, the numerical values of T^* are slightly bigger than in experiment, but show the same curvature. In Fig. 2 (d), we supplement a power fit $T^* \propto B_{\mathrm{ext}}^{-\alpha}$ to the numerical data. Like in the experimental results, the best agreement was achieved for $\alpha = 0.7$. Deviations from the power law with $\alpha = 1$ can be attributed to the importance of the hyperfine interaction and the electronic spin-spin interaction at lower magnetic fields.

These results will open the door for a new quest to determine the microscopic origin of the effective interaction. While a direct exchange interaction or a dipole-dipole interaction are too weak due to the typical QD distance of 100 nm, an indirect RKKY interaction mediated by carriers in the wetting layer is a potential candidate. Additional information

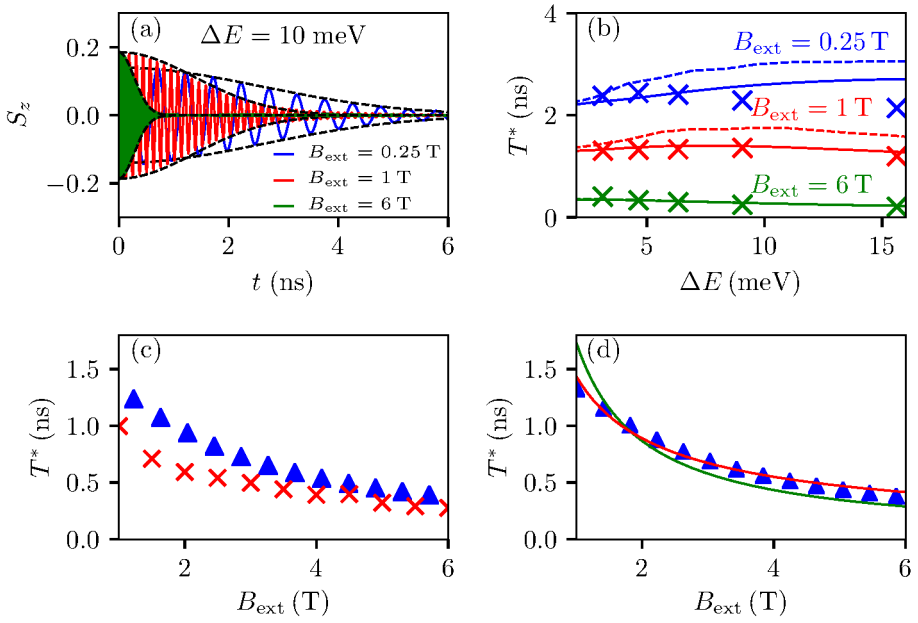

Figure 2. (a) Dephasing of the electron spin polarisation at different magnetic fields. (b) Dephasing time T^* as function of the spectral laser width ΔE. In addition to the numerical results after a single pulse (solid lines) and experimental data (x markers), we added the calculations after 100 pulses (dashed lines). (c) Dependence of T^* on the external magnetic field $B_{\rm ext}$. Experimental data (x markers) and numerical results (triangles) are presented. (d) The data points of the numerical calculation (triangles) are compared to a dependency $\propto 1/B_{\rm ext}^{\alpha}$ with $\alpha = 1$ (green curve) and $\alpha = 0.7$ (red curve).

about the inter QD interaction might enable the design of pulse sequences in multi-colon setups that generate tailored quantum states and pave the way to quantum functionality.

4 Magnetic Field Dependence of the Electron Spin Revival Amplitude in Periodically Pulsed Quantum Dots

During a periodic pulse sequence with repetition time T_R, first the electron spin synchronises with the optical excitation and a purely electronic revival with an amplitude of approx. 0.077 evolves (see Fig. 3 (a) orange curve). As a consequence of the continuous periodic pulsing, the nuclear spins start to align generating a non-equilibrium Overhauser field distribution. The initially Gaussian distribution (dashed blue line in Fig. 3 (b)) transforms into a peaked structure (red curve). In combination with the external magnetic field, the Overhauser field enables either an integer or a half-integer number of electron revolutions between two pump pulses. In case of the external magnetic field $B_{\rm ext} = 1.95$ T for example, the peaks in the Overhauser field distribution correspond to an integer number of electron revolutions (indicated by gray dashed vertical lines). As a result of the non-equilibrium Overhauser field distribution, the electron spin revival amplitude either increases or de-

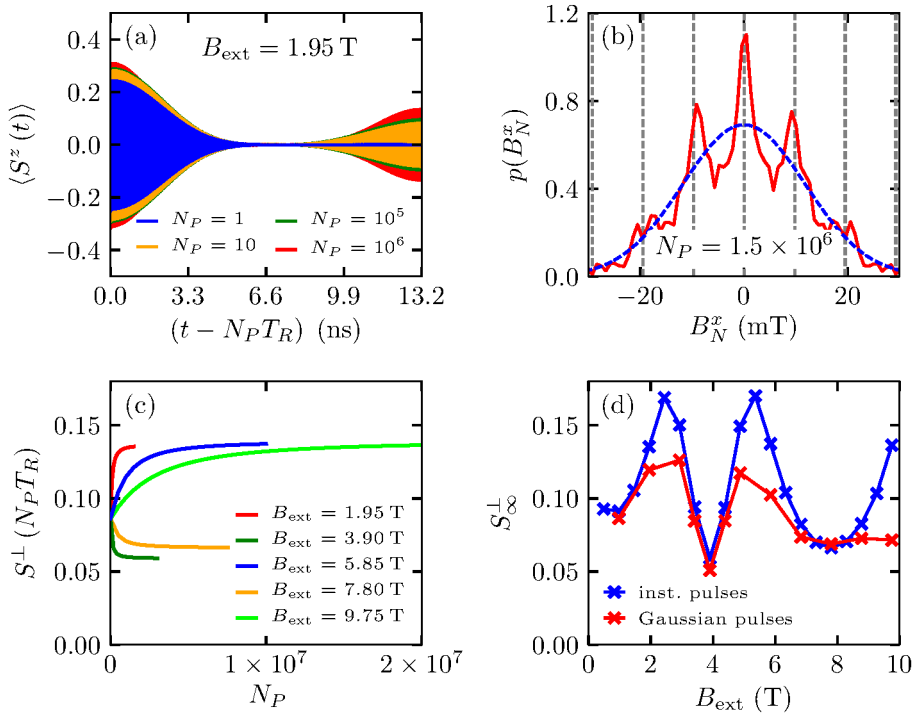

Figure 3. Evolution of electron spin polarisation $\langle S^z \rangle$ between two laser pulses. For $B_{\rm ext} = 1.95\,\mathrm{T}$ the revival grows due to the aligning of nuclear spins during the pulse sequence. (b) The Overhauser field distribution $p(B_N^x)$ along the magnetic field $B_{\rm ext} = 1.95\,\mathrm{T}$ leads to an integer number of electron revolutions during T_R. (c) The evolution of the revival amplitude $S^\perp(N_P T_R)$ with increasing number N_P of instantaneous optical pulses depends on $B_{\rm ext}$ and the peak structure evolving in $p(B_N^x)$. (d) Steady-state revival amplitude as function of the external magnetic field. The blue/red data points correspond to instantaneous/Gaussian laser pulses, respectively.

creases starting from the initial electronic value, as depicted in Fig. 3 (c). The speed of revival amplitude modification depends on the number of nuclear spin revolutions during the period T_R. At $B_{\rm ext} = 1.95$ T, for instance, the nuclear spins perform a quarter turn in between laser pulses. Due to the different resonance conditions, the steady-state amplitude reached after several million pump pulses in Fig. 3 (d) displays a non-monotonic behaviour as function of the external magnetic field.[12]

For different types of laser pulses employed in the simulation, instantaneous or Gaussian resonant π pulses, the electron revival is more or less efficiently generated. In case of instantaneous pulses the electron spin up state population is completely transferred to the trion state and thereupon decays. The longer the pulse duration becomes (or the stronger the external magnetic field is), the more revolutions the electron spin performs during the pulse which renders the pumping inefficient. This mechanism also yields a smaller revival amplitude for Gaussian pulses with 6 ps width especially for strong magnetic fields (see Fig. 3(d)).

The simulations with our quantum mechanical approach suited for long pulse sequences bring comprehension of experimental observations[12] that the revival amplitude displays a pronounced minimum at 4 T. The magnetic field dependence is even more complex in experiment due to different nuclear species with distinct resonance conditions that lead to a superimposed behaviour for the electron revival.

5 Concluding Remarks

We reported on our recent studies on singly-charged semiconductor quantum dots under optical excitation. We tackle the problem from two angles of view to analyse the nuclear induced frequency focusing effect that significantly enhances the spin coherence time as well as the long-range spin-spin interaction that enables information transfer between quantum dots. A numerically exact quantum approach is used to simulate several million laser pulses. By analysis of the resonance condition in the periodically driven system we explain the non-monotonic magnetic-field dependence of the revival amplitude observed in recent experiments.

Since the quantum approach is limited to a small number of spins, we utilise a semi-classical approach to simulate coupled clusters of quantum dots. The additional electronic spin-spin interaction that is incorporated in our cluster approach explains the dephasing time that is independent of the spectral laser width in experiment on quantum dot ensembles. Further investigations of the long-range spin-spin interaction might reveal the physical mechanism behind the effective coupling in the cluster approach.

Acknowledgements

This project was supported by the Deutsche Forschungsgemeinschaft through the transregio TRR 160 within the Projects No. A4 and No. A7. The authors gratefully acknowledge the computing time granted by the John von Neumann Institute for Computing (NIC) and provided for project HDO09 on the supercomputer JURECA at Jülich Supercomputing Centre (JSC). Furthermore, the authors gratefully acknowledge the Gauss Centre for Supercomputing e.V. (`www.gauss-centre.eu`) for funding this project by providing computing time through the NIC on the GCS Supercomputers JUQUEEN and JUWELS at JSC.

References

1. W. Beugeling, G. S. Uhrig, and F. B. Anders, *Quantum model for mode locking in pulsed semiconductor quantum dots*, Phys. Rev. B **94**, 245308, 2016.
2. W. Beugeling, G. S. Uhrig, and F. B. Anders, *Influence of the nuclear Zeeman effect on mode locking in pulsed semiconductor quantum dots*, Phys. Rev. B **96**, 115303, 2017.
3. N. Jäschke, A. Fischer, E. Evers, V. V. Belykh, A. Greilich, M. Bayer, and F. B. Anders, *Nonequilibrium nuclear spin distribution function in quantum dots subject to periodic pulses*, Phys. Rev. B **96**, 205419, 2017.

4. A. Greilich, D. R. Yakovlev, A. Shabaev, Al. L. Efros, I. A. Yugova, R. Oulton, V. Stavarache, D. Reuter, A. Wieck, and M. Bayer, *Mode Locking of Electron Spin Coherences in Singly Charged Quantum Dots*, Science **313**, 341–345, 2006.
5. A. Greilich, A. Shabaev, D. R. Yakovlev, Al. L. Efros, I. A. Yugova, D. Reuter, A. D. Wieck, and M. Bayer, *Nuclei-Induced Frequency Focusing of Electron Spin Coherence*, Science **317**, 1896–1899, 2007.
6. N. Jäschke, F. B. Anders, and M. M. Glazov, *Electron spin noise under the conditions of nuclei-induced frequency focusing*, Phys. Rev. B **98**, 045307, 2018.
7. S. Spatzek, A. Greilich, Sophia E. Economou, S. Varwig, A. Schwan, D. R. Yakovlev, D. Reuter, A. D. Wieck, T. L. Reinecke, and M. Bayer, *Optical Control of Coherent Interactions between Electron Spins in InGaAs Quantum Dots*, Phys. Rev. Lett. **107**, 137402, 2011.
8. R. Hanson, L. P. Kouwenhoven, J. R. Petta, S. Tarucha, and L. M. K. Vandersypen, *Spins in few-electron quantum dots*, Rev. Mod. Phys. **79**, 1217–1265, 2007.
9. I. A. Merkulov, Al. L. Efros, and M. Rosen, *Electron spin relaxation by nuclei in semiconductor quantum dots*, Phys. Rev. B **65**, 205309, 2002.
10. M. I. Dyakonov, *Spin Physics in Semiconductors*, Springer Series in Solid-State Sciences **157**, Springer-Verlag Berlin Heidelberg, 2008.
11. M. Gaudin, *Diagonalisation d'une classe d'hamiltoniens de spin*, J. Physique **37**, 1087, 1976.
12. I. Kleinjohann, E. Evers, P. Schering, A. Greilich, G. S. Uhrig, M. Bayer, and F. B. Anders, *Magnetic field dependence of the electron spin revival amplitude in periodically pulsed quantum dots*, Phys. Rev. B **98**, 155318, 2018.
13. G. Chen, D. L. Bergman, and L. Balents, *Semiclassical dynamics and long-time asymptotics of the central-spin problem in a quantum dot*, Phys. Rev. B **76**, 045312, 2007.
14. A. Fischer, E. Evers, S. Varwig, A. Greilich, M. Bayer, and F. B. Anders, *Signatures of long-range spin-spin interactions in an (In,Ga)As quantum dot ensemble*, Phys. Rev. B **98**, 205308, 2018.
15. A. Greilich, D. R. Yakovlev, and M. Bayer, *Optical tailoring of electron spin coherence in quantum dots*, Solid State Communications **49**, 1466–1471, 2009.